VIP Porous Crystals Very Important Paper

International Edition: DOI: 10.1002/anie.201916397
German Edition: DOI: 10.1002/ange.201916397

Monolayer Two-dimensional Molecular Crystals for an Ultrasensitive OFET-based Chemical Sensor

*Haiyang Li, Yanjun Shi, Guangchao Han, Jie Liu, Jing Zhang, Chunlei Li, Jie Liu, Yuanping Yi, Tao Li, Xike Gao, Chongan Di, Jia Huang, Yanke Che, Dong Wang, Wenping Hu, Yunqi Liu, and Lang Jiang**

Abstract: *The sensitivity of conventional thin-film OFET-based sensors is limited by the diffusion of analytes through bulk films and remains the central challenge in sensing technology. Now, for the first time, an ultrasensitive (sub-ppb level) sensor is reported that exploits n-type monolayer molecular crystals (MMCs) with porous two-dimensional structures. Thanks to monolayer crystal structure of NDI3HU-DTYM2 (NDI) and controlled formation of porous structure, a world-record detection limit of NH_3 (0.1 ppb) was achieved. Moreover, the MMC-OFETs also enabled direct detection of solid analytes of biological amine derivatives, such as dopamine at an extremely low concentration of 500 ppb. The remarkably improved sensing performances of MMC-OFETs opens up the possibility of engineering OFETs for ultrasensitive (bio)chemical sensing.*

Organic two-dimensional (2D) semiconductor materials have brought unprecedented impact on materials science, physics, chemistry, and industry,[1] since the emergence of monolayer crystalline active layer in organic field-effect transistors (OFETs).[1a,2] The charge density and charge transportation in the conducting channel of OFETs are not only modulated by gate bias, but also dominated by external stimulus, such as presence of specific chemicals, enabling their capability of chemical sensing.[2d,3] Moreover, OFET-based sensors, where the OFETs act as both signal transducers and signal amplifiers, substantially simplified the structure of traditional sensing devices. However, the sensing performances of thin film OFET-based sensors are limited by the diffusion process of analyte molecules to the conducting channels.[3e,4] To improve the sensing performances, many efforts have been devoted to alleviate the diffusion barrier by either introducing porous structure into organic semiconductor (OSC) films[3e,5] or decreasing the film thickness down to a few layers[6] or even monolayers.[3b,f,7]

Recently, exciting progress has been achieved regarding the OFET-based sensors for ammonia detection,[8] not only because it is of crucial importance for environmental protection purpose, but also ammonia is a biochemical clue for cirrhotic disease or chronic kidney disease.[9] Huang et al. reported OFET-based NH_3 sensors by exploiting p-type OSCs, since the electrostatic interaction between NH_3 and OSCs can lead to the decrease in current, with a detection limit up to 350 ppb (as summarized in the Supporting Information, Table S1).[8b] Further improvement over the detection limit (that is, ca. 10 ppb) was achieved by decreasing the thickness of semiconductor layer to few molecular layers, for example, monolayer films[3f,8g] and monolayer molecular crystals (MMCs).[8g] On the other hand, introducing porous structure was also shown to be an alternative strategy to tailor the sensitivity, which have enabled the NH_3 detection limit of 1–10 ppb.[3e,5c] However, direct preparation of porous two-dimensional molecular crystals by the bottom-up assembly process is still very scarce for ultrasensitive NH_3 sensing.

Herein, we report an n-type OFET-based MMCs for NH_3 detection, by in situ forming of a porous structure. Since NH_3 molecules exhibit five times higher binding affinity to the core of NDI3HU-DTYM2[10] (NDI, Figure 1 a) than its side groups (Supporting Information, Figure S1), the porous structure is expected to significantly improve the sensitivity and detection

[*] H. Y. Li, Y. J. Shi, G. C. Han, Prof. J. Liu, J. Zhang, C. L. Li, Dr. J. Liu, Prof. Y. P. Yi, Prof. C. A. Di, Prof. Y. K. Che, Prof. D. Wang, Prof. Y. Q. Liu, Prof. L. Jiang
Beijing National Laboratory for Molecular Sciences, Institute of Chemistry, Chinese Academy of Sciences
University of Chinese Academy of Sciences
Beijing 100190 (China)
E-mail: ljiang@iccas.ac.cn

Prof. T. Li
School of Chemistry and Chemical Engineering and Key Laboratory of Thin Film and Microfabrication (Ministry of Education)
Shanghai Jiao Tong University
Shanghai 200240 (China)

Prof. X. K. Gao
Key Laboratory of Synthetic and Self-Assembly Chemistry for Organic Functional Molecules, Center for Excellence in Molecular Synthesis, Shanghai Institute of Organic Chemistry, Shanghai Institute of Organic Chemistry, Chinese Academy of Sciences
Shanghai 200032 (China)

Prof. J. Huang
Interdisciplinary Materials Research Center
School of Materials Science and Engineering
Tongji University, Shanghai 201804 (China)

Prof. W. P. Hu
Tianjin Key Laboratory of Molecular Optoelectronic Sciences, Department of Chemistry, School of Science, Tianjin University
Tianjin 300072 (China)

Supporting information and the ORCID identification number(s) for the author(s) of this article can be found under: https://doi.org/10.1002/anie.201916397.

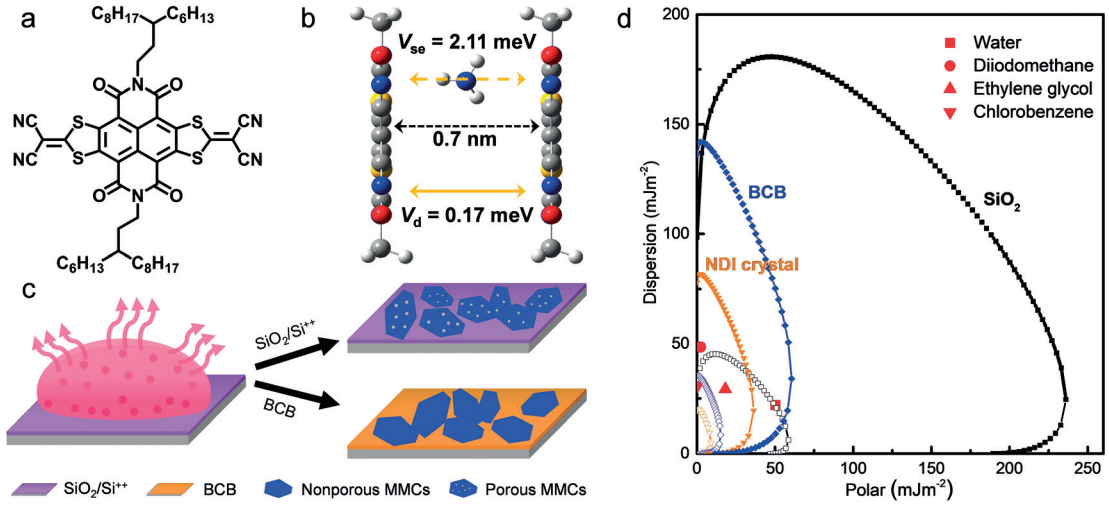

Figure 1. a) Chemical structure of NDI3HU-DTYM2 (NDI). b) The intermolecular direct electronic coupling (V_d) and long-range super-exchange coupling (V_{se}) with inserted an ammonia between two NDI molecules. c) Illustration of the preparation of MMCs. d) Wetting envelopes of BCB, plasma treated SiO_2/Si^{++} substrates, and crystals of NDI at 0° (hollow symbol line) and 90° (solid symbol line).

limit. The calculated results indicate that the absorbed ammonia between long-distance NDI molecules can lead to an important long-range super-exchange coupling and thus improve the charge-transport performance (Figure 1b; Supporting Information, Figure S2). The as-prepared porous OFET-based sensors demonstrated a record NH_3 detection limit (0.1 ppb). Moreover, the OFET-based MMCs were further extended to the sensing of solid amine-derivatives, that is, dopamine, with a detection limit up to 500 ppb, corroborating the versatility of these OFET-based chemical sensors. These results open up the possibility of constructing the next generation high-performance sensing devices with high resolution for industrial gas detection or biological diagnosis.

A simple drop-casting strategy was employed to realize the controllable tuning of the structural parameters, that is, monolayer or multiple-layer; porous or nonporous structure; pore sizes. As illustrated in Figure 1c, 5–30 μL NDI in chlorobenzene with different concentrations were drop-casted onto the surface of plasma-treated SiO_2/Si^{++} or divinyltetramethylsiloxanebis (benzocyclobutene) derivative (BCB)-treated SiO_2/Si^{++} substrates. After the solvent evaporation, films with regular shapes were obtained under ambient conditions (Figure 2,b). Crystal films were confirmed by their homogeneous brightness under polarized illumination (Supporting Information, Figure S3).

The thickness of the crystals is assessed by atomic force microscopy (AFM), and the thicknesses of these samples are 1.8–2.1 nm, as shown in Figure 2c,d, which correlates to the thickness of monolayer height of the lamellar films reported,[8c] indicating the formation of monolayer crystals. On the other hand, the NDI multilayer crystals were also evidenced by the *h*00 peaks in X-ray diffraction patterns (Supporting Information, Figure S4), which corresponded to a layer-by-layer growth manner. The d-spacing is 2.08 nm, which is approximately or is slightly larger than the thickness of the ultrathin crystals, further confirming the monolayer thickness of the ultrathin crystals. In contrast the smooth morphology obtained on BCB/SiO_2/Si^{++}, nanopores were clearly observed

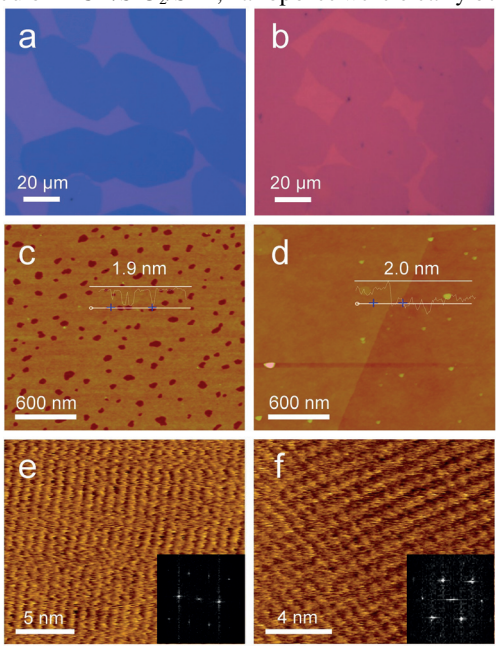

Figure 2. a),b) Optical microscope images, c),d) AFM images, and e),f) HR-AFM images of MMCs obtained on SiO_2/Si^{++} (left) and BCB/SiO_2/Si^{++} (right) substrates, respectively.

for crystals grown on SiO_2/Si^{++}. However, the packing motifs of these MMCs were similar, as evidenced by the high-resolution atomic force microscope (HR-AFM), where similar packing parameters of $a = 9.34$ Å, $b = 7.39$ Å, $\theta = 74.67°$ and $a = 9.71$ Å, $b = 7.39$ Å, $\theta = 73.49°$ are extracted for the porous and nonporous MMCs (Figure 2e,f). The thickness and size of the pores of MMCs can also be tuned by changing the C_{NDI} (Supporting Information, Figures S5–S8).

To reveal the reliance of NDI MMCs morphologies on the substrates, surface free energies of the NDI crystals and the substrates were investigated. The wetting envelopes are

shown in Figure 1d.[11] Chlorobenzene exhibited similar wettability to the NDI crystal and the BCB substrates, resulting in a steady solvent receding effect during the crystal growth at the BCB substrates/NDI nucleus interface. Therefore, homogenous and smooth MMCs were obtained (Figure 2b). By contrast, large difference between wettability of chlorobenzene on NDI crystal and the SiO_2/Si^{++} would result in unsteady solvent receding line at the SiO_2/crystal nucleus interface, which could lead to the formation of porous structure (Figure 2a). As we claimed, the porous MMCs formed on SiO_2/Si^{++} can provide great opportunity for fabricating ultra-high-performance gas sensors based on OFET devices (Supporting Information, Figure S9).

To probe its sensing performance of NH_3 detecting, the changes in the output current were recorded in the sampling mode. In our work herein, the porous MMC-OFETs experienced a 120% current increase upon exposure to 1 ppb NH_3. Plot of $(I-I_0)/I_0$ against NH_3 concentration (from 1 ppb to 1% (v/v) (diluted by N_2)) is further summarized in Figure 3a and the Supporting Information, Figure S10, for both porous and nonporous MMC-OFETs. As shown in Figure 3a and Figure S10, the current gradually increased with the increase of the C_{NH_3} and then leveled off when it reached 1 ppm. To probe the detection limit of MMC-OFETs at 0.1 ppb, the porous device suddenly underwent a current increase of 72%, while no current variation was observed for the nonporous MMC-OFETs (Figure 3b). To the best of our knowledge, this is the first report achieving a sub-ppb level NH_3 detection by OFETs based sensors (Supporting Information, Table S1).

While the nonporous MMC-OFETs only exhibited 73% response after 1 ppb NH_3 exposure and the I_D kept increasing with higher C_{NH_3}. An upper sensing limit was not detected at the whole testing C_{NH_3} range, which may complement the porous MMC-OFETs for higher C_{NH_3} sensing. The porous device exhibited superior sensitivity than the nonporous device through the whole testing C_{NH_3} range (Figure 3a). Moreover, further to the substantially improved sensitivity, the response of porous MMCs was faster than that of the nonporous MMCs (Supporting Information, Figure S11).

For comparison, the sensing performances of multilayer crystals OFET were also studied, which only showed about 1.8% and 3.2% I_D increase at C_{NH_3} of 10 ppm and 100 ppm (Supporting Information, Figure S12). Apart from the outstanding sensing property of the porous MMCs, the effect of the pore size to the sensitivity was also investigated (Supporting Information, Figure S13). The sensitivity was enhanced when the pore diameter increased from 20 to 200 nm. The selectivity studies of porous MMC-OFET sensors were carried out by exposing the MMC-OFETs devices to those chemical vapors including isopropanol, acetone, alcohol,

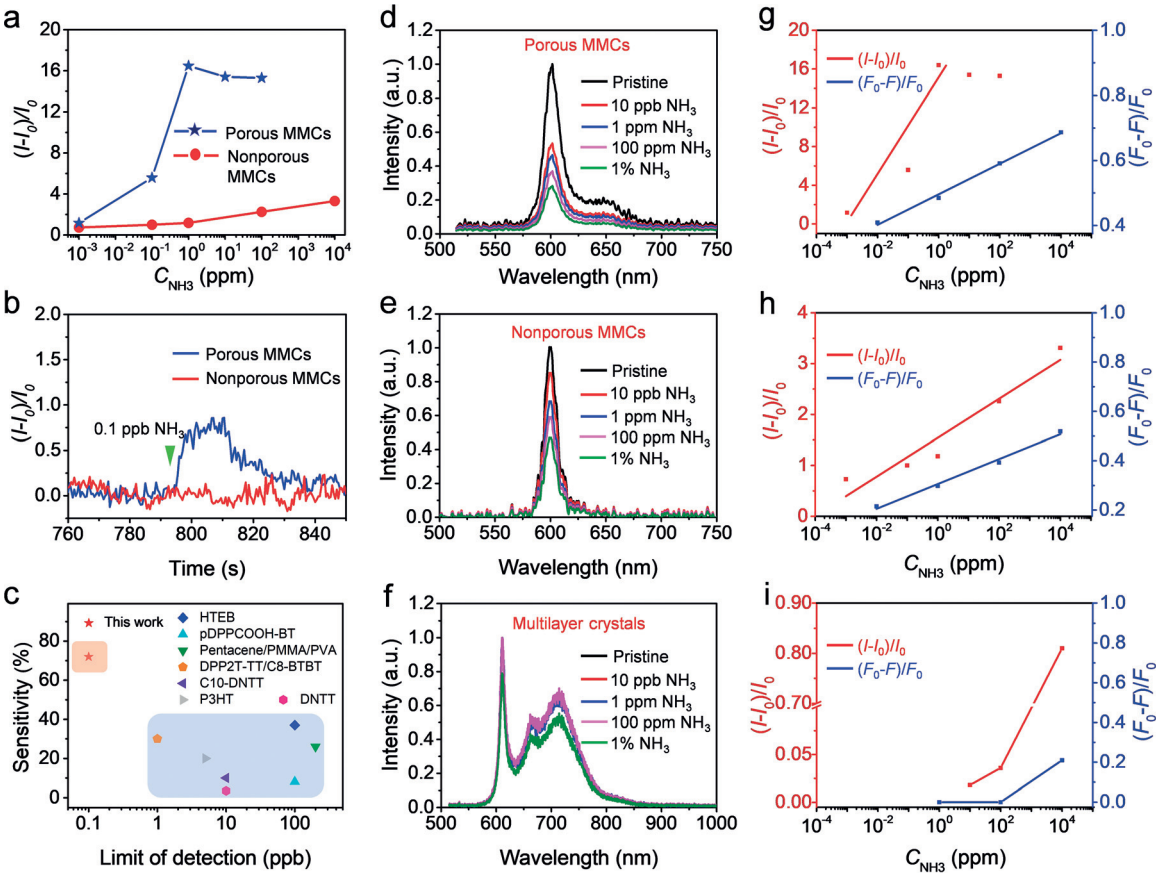

Figure 3. Performances of MMC-OFET-based gas sensors. a) The sensitivity and b) the current responses (0.1 ppb NH_3) of the porous and nonporous MMC-OFETs based sensors. c) The limit of detection and sensitivity of porous MMCs in comparison with reported sensors. d)–f) Variation of normalized FL intensity of porous, nonporous MMCs, and multilayer crystals after exposure to ammonia vapors at concentration ranging from 10 ppb to 1%. g)–i) The variation of fluorescence intensity, and OFET-based sensor performance of porous, nonporous MMCs, and multilayer crystals.

THF, and chloroform (Supporting Information, Figure S14). Only a slight increase in current was detected for those volatile organic compounds even at saturated concentrations at 25 °C. The outstanding sensitivity and high selectivity of the sensors toward NH_3 proved the great potential of porous MMC-OFETs in sensing applications.

Besides the electrical study based on OFETs, the interaction between NH_3 molecules and NDI MMCs was investigated by fluorescent (FL) spectra. Figure 3d shows the variation of FL spectra of the porous MMCs after exposure to NH_3 vapors at concentrations ranging from 10 ppb to 1% (normalized by the pristine intensity at 601 nm). Control experiments were carried on the nonporous MMCs (Figure 3e) and multilayer crystals (Figure 3f). The FL intensity of NDI MMCs decreased obviously after NH_3 exposure. Figure 3g–i shows the relative FL intensity at 601 nm vs. $\log C_{NH_3}$, and the decrease of FL intensity is linearly related to the increase of ammonia concentration on semilog coordinates. This relationship is consistent with that of the electrical results of OFET-based sensors, but the current change is more obvious than the FL in sensing NH_3 with lower detection limit and higher sensitivity. For example, at 1 ppm of NH_3 the sensitivity of electrical signal of the porous MMCs sensors is about 34 times higher than that of FL signal. All the slops of liner fitting are extracted and summarized in the Supporting Information, Table S2. In the case of multilayer crystals, the FL intensity almost kept unchanged until ammonia concentration exceeded 1%, owing to the bulk thickness and the low percentage of the interfacial molecules to the bulk crystals. The FL spectral study further confirmed the superiority of porous MMCs toward nonporous MMCs and bulk crystals in gas sensors applications. It is noted that the slope of sensitivity vs. log C_{NH3} of electronic signal of porous MMCs was about 100 times higher than the spectroscopic slope, and that of nonporous MMCs was 8 times higher than the spectroscopic slope, demonstrating the high resolution of the electrical sensors at low NH_3 concentration.

In the previous study of OFET-based sensors, the detection of solid chemicals is limited by the diffusion process of the solid analytes.[12] However, the direct exposure of the charge accumulation layer in MMC-OFETs provides the possibility of sensing solid chemicals. In this work, dopamine powders were used as the solid chemical to evaluate the sensing property of MMC-OFETs toward solid analytes. As shown in Figure 4a, obvious current increase can be observed for the nonporous MMC devices upon exposure to dopamine powders diluted by silicon powders. This device shows 758% current increase when 500 ppb (*m*/*m*) dopamine was added. The porous NDI MMC device also showed obvious response under the same condition, as shown in Figure 4b. We also compared the sensing performance of the multilayer crystal OFET based sensors. As shown in the Supporting Information, Figure S15, the sensors of multilayer crystal OFETs exhibited negligible response under the same condition. The results indicate that monolayer thickness of the conduction channel is playing an important role in sensing solid chemicals.

In summary, MMCs with different morphologies were controllably synthesized and their application in sensors were investigated by fabricating MMC-OFETs. Sensors of porous MMCs exhibited high sensitivity toward NH_3 with 72% response at 0.1 ppb NH_3, which is the record of OFET-based NH_3 sensors so far reported. Besides, both electrical and fluorescent change were detected when exposing to NH_3, while the sensitivity of electrical signal of the porous MMCs sensor is about 34 times higher than that of FL signal. Moreover, the direct detection of solid chemicals was firstly demonstrated based on the MMC-OFETs, and the sensor showed obvious response to sub-ppm level of dopamine powders. The easy preparation of MMCs and ultra-sensitivity of the MMC-OFETs based sensors might render further application for real-time detection of gas and solid chemicals.

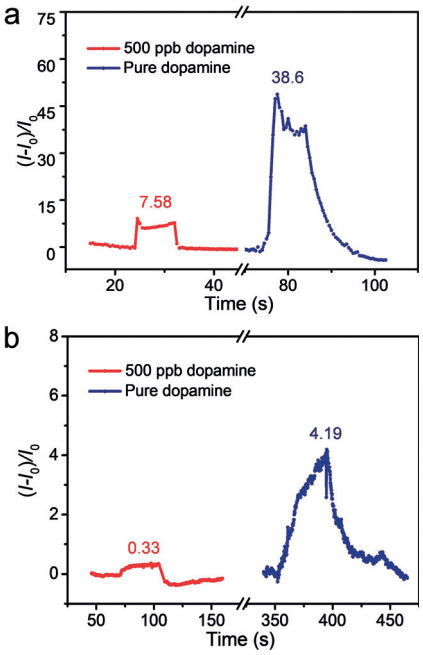

Figure 4. The current responses of a) nonporous and b) porous MMCs sensors upon exposure to dopamine powders at concentrations of 500 ppb and pure dopamine.

Acknowledgements

We thanks to Prof. Ji Liu for the discussion. This work was supported by the Ministry of Science and Technology of China (2016YFB0401100, 2017YFA0204704), the National Natural Science Foundation of China (21873108, 21805284, 51673114, 51973111), the Chinese Academy of Sciences (Hundred Talents Plan, Youth Innovation Promotion Association), the Strategic Priority Research Program (Grant No. XDB30000000).

Conflict of interest

The authors declare no conflict of interest.

Keywords: monolayer molecular crystals (MMCs) · organic field-effect transistors (OFETs) · porous crystals · sensors

How to cite: *Angew. Chem. Int. Ed.* **2020**, *59*, 4380–4384
Angew. Chem. **2020**, *132*, 4410–4414

[1] a) L. Jiang, H. Dong, Q. Meng, H. Li, M. He, Z. Wei, Y. He, W. Hu, *Adv. Mater.* **2011**, *23*, 2059–2063; b) L. Jiang, H. Dong, Q. Meng, J. Tan, W. Jiang, C. Xu, Z. Wang, W. Hu, *Adv. Mater.* **2012**, *24*, 694–698; c) C. Wang, X. Ren, C. Xu, B. Fu, R. Wang, X. Zhang, R. Li, H. Li, H. Dong, Y. Zhen, S. Lei, L. Jiang, W. Hu, *Adv. Mater.* **2018**, *30*, 1706260; d) Y. Shi, L. Jiang, J. Liu, Z. Tu, Y. Hu, Q. Wu, Y. Yi, E. Gann, C. R. McNeill, H. Li, W. Hu, D. Zhu, H. Sirringhaus, *Nat. Commun.* **2018**, *9*, 2933; e) J. Liu, L. Jiang, W. Hu, Y. Liu, D. Zhu, *Sci. Chin. Chem.* **2019**, *62*, 313–330; f) Q. Wang, J. Qian, Y. Li, Y. Zhang, D. He, S. Jiang, Y. Wang, X. Wang, L. Pan, J. Wang, X. Wang, Z. Hu, H. Nan, Z. Ni, Y. Zheng, Y. Shi, *Adv. Funct. Mater.* **2016**, *26*, 3191–3198; g) D. He, J. Qiao, L. Zhang, J. Wang, T. Lan, J. Qian, *Sci. Adv.* **2017**, *3*, e1701186; h) C. Xu, P. He, J. Liu, A. Cui, H. Dong, Y. Zhen, W. Chen, W. Hu, *Angew. Chem. Int. Ed.* **2016**, *55*, 9519–9523; *Angew. Chem.* **2016**, *128*, 9671–9675; i) L. Li, P. Gao, W. Wang, K. Mullen, H. Fuchs, L. Chi, *Angew. Chem. Int. Ed.* **2013**, *52*, 12530–12535; *Angew. Chem.* **2013**, *125*, 12762–12767; j) S. Wu, M. Li, H. Phan, D. Wang, T. S. Herng, J. Ding, Z. Lu, J. Wu, *Angew. Chem. Int. Ed.* **2018**, *57*, 8007–8011; *Angew. Chem.* **2018**, *130*, 8139–8143; k) J. Adisoejoso, K. Tahara, S. Okuhata, S. Lei, Y. Tobe, S. De Feyter, *Angew. Chem. Int. Ed.* **2009**, *48*, 7353–7357; *Angew. Chem.* **2009**, *121*, 7489–7493.

[2] a) H. Sirringhaus, *Adv. Mater.* **2014**, *26*, 1319–1335; b) Y. Guo, G. Yu, Y. Liu, *Adv. Mater.* **2010**, *22*, 4427–4447; c) G. Gelinck, P. Heremans, K. Nomoto, T. D. Anthopoulos, *Adv. Mater.* **2010**, *22*, 3778–3798; d) C. Zhang, P. Chen, W. Hu, *Chem. Soc. Rev.* **2015**, *44*, 2087–2107; e) C. Wang, H. Dong, L. Jiang, W. Hu, *Chem. Soc. Rev.* **2018**, *47*, 422–500; f) H. Jiang, W. Hu, *Angew. Chem. Int. Ed.* **2020**, *59*, 1408–1428; *Angew. Chem.* **2020**, *132*, 1424–1445; g) J. Yin, Y. Zhou, T. Lei, J. Pei, *Angew. Chem. Int. Ed.* **2011**, *50*, 6320–6323; *Angew. Chem.* **2011**, *123*, 6444–6447; h) M. Li, H. Bin, X. Jiao, M. M. Wienk, H. Yan, R. A. J. Janssen, *Angew. Chem. Int. Ed.* **2020**, *59*, 846–852; *Angew. Chem.* **2020**, *132*, 856–862; i) Y. Cao, Z. Wei, S. Liu, L. Gan, X. Guo, W. Xu, M. L. Steigerwald, Z. Liu, D. Zhu, *Angew. Chem. Int. Ed.* **2010**, *49*, 6319–6323; *Angew. Chem.* **2010**, *122*, 6463–6467.

[3] a) H. Li, W. Shi, J. Song, H. J. Jang, J. Dailey, J. Yu, H. E. Katz, *Chem. Rev.* **2019**, *119*, 3–35; b) X. Wu, S. Mao, J. Chen, J. Huang, *Adv. Mater.* **2018**, *30*, 1705642; c) T. Someya, A. Dodabalapur, J. Huang, K. C. See, H. E. Katz, *Adv. Mater.* **2010**, *22*, 3799–3811; d) C. A. Di, F. Zhang, D. Zhu, *Adv. Mater.* **2013**, *25*, 313–330; e) J. Lu, D. Liu, J. Zhou, Y. Chu, Y. Chen, X. Wu, J. Huang, *Adv. Funct. Mater.* **2017**, *27*, 1700018; f) S. Zhang, Y. Zhao, X. Du, Y. Chu, S. Zhang, J. Huang, *Small* **2019**, *15*, 1805196.

[4] a) G. Horowitz, *J. Mater. Res.* **2004**, *19*, 1946–1962; b) X. Sun, Y. Liu, C. A. Di, Y. Wen, Y. Guo, L. Zhang, Y. Zhao, G. Yu, *Adv. Mater.* **2011**, *23*, 1009–1014; c) A. Di, Y. Liu, G. Yu, D. Zhu, *Acc. Chem. Res.* **2009**, *42*, 1573–1583.

[5] a) B. Kang, M. Jang, Y. Chung, H. Kim, S. K. Kwak, J. H. Oh, K. Cho, *Nat. Commun.* **2014**, *5*, 4752; b) Y. Yang, G. Zhang, H. Luo, J. Yao, Z. Liu, D. Zhang, *ACS Appl. Mater. Interfaces* **2016**, *8*, 3635–3643; c) F. Zhang, G. Qu, E. Mohammadi, J. Mei, Y. Diao, *Adv. Funct. Mater.* **2017**, *27*, 1701117.

[6] a) J. Huang, J. Sun, H. E. Katz, *Adv. Mater.* **2008**, *20*, 2567–2572; b) J. Yu, X. Yu, L. Zhang, H. Zeng, *Sens. Actuators B* **2012**, *173*, 133–138; c) X. Yu, N. Zhou, S. Han, H. Lin, D. Buchholz, J. Yu, H. R. Chang, J. T. Marks, A. Facchetti, *J. Mater. Chem. C* **2013**, *1*, 6532–6535; d) L. Li, P. Gao, M. Baumgarten, K. Mullen, N. Lu, H. Fuchs, L. Chi, *Adv. Mater.* **2013**, *25*, 3419–3425.

[7] a) C. Anichini, W. Czepa, D. Pakulski, A. Aliprandi, A. Ciesielski, P. Samori, *Chem. Soc. Rev.* **2018**, *47*, 4860–4908; b) A. A. Trul, A. S. Sizov, V. P. Chekusova, O. V. Borshchev, E. V. Agina, M. A. Shcherbina, A. V. Bakirov, S. N. Chvalun, S. A. Ponomarenko, *J. Mater. Chem. C* **2018**, *6*, 9649–9659; c) A. S. Sizov, A. A. Trul, V. Chekusova, O. V. Borshchev, A. A. Vasiliev, E. V. Agina, S. A. Ponomarenko, *ACS Appl. Mater. Interfaces* **2018**, *10*, 43831–43841.

[8] a) X. Zhuang, D. Zhang, X. Wang, X. Yu, J. Yu, *Appl. Phys. Lett.* **2018**, *113*, 263301; b) W. Huang, K. Besar, R. LeCover, A. M. Rule, P. N. Breysse, H. E. Katz, *J. Am. Chem. Soc.* **2012**, *134*, 14650–14653; c) F. Zhang, C. A. Di, N. Berdunov, Y. Hu, Y. Hu, X. Gao, Q. Meng, H. Sirringhaus, D. Zhu, *Adv. Mater.* **2013**, *25*, 1401–1407; d) Q. Meng, F. Zhang, Y. Zang, D. Huang, Y. Zou, J. Liu, G. Zhao, Z. Wang, D. Ji, C. A. Di, W. Hu, D. Zhu, *J. Mater. Chem. C* **2014**, *2*, 1264–1269; e) S. Han, X. Zhuang, Y. Jiang, X. Yang, L. Li, J. Yu, *Sens. Actuators B* **2017**, *243*, 1248–1254; f) M. Mirza, J. Wang, D. Li, S. A. Arabi, C. Jiang, *ACS Appl. Mater. Interfaces* **2014**, *6*, 5679–5684; g) B. Peng, S. Huang, Z. Zhou, P. K. L. Chan, *Adv. Funct. Mater.* **2017**, *27*, 1700999.

[9] a) R. Adrover, D. Cocozzella, E. Ridruejo, A. Garcia, J. Rome, J. J. Podesta, *Dig. Dis. Sci.* **2012**, *57*, 189–195; b) S. J. Davies, P. Španěl, D. Smith, *Bioanalysis* **2014**, *6*, 843–857; c) X. Xiao, X. F. Cheng, X. Hou, J. H. He, Q. F. Xu, H. Li, N. J. Li, D. Y. Chen, J. M. Lu, *Small* **2017**, *13*, 1602190; d) J. Zhou, H. Lin, X. F. Cheng, J. Shu, J. H. He, H. Li, Q. F. Xu, N. J. Li, D. Y. Chen, J. M. Lu, *Mater. Horiz.* **2019**, *6*, 554–562.

[10] a) Y. Hu, Y. Qin, X. Gao, F. Zhang, C. A. Di, Z. Zhao, H. Li, D. Zhu, *Org. Lett.* **2012**, *14*, 292–295; b) Y. Hu, X. Gao, C. A. Di, X. Yang, F. Zhang, Y. Liu, H. H. Li, D. Zhu, *Chem. Mater.* **2011**, *23*, 1204–1215; c) X. Gao, C. A. Di, Y. Hu, X. Yang, H. Fan, F. Zhang, Y. Liu, H. Li, D. Zhu, *J. Am. Chem. Soc.* **2010**, *132*, 3697–3699.

[11] a) R. O. F. Verkuijlen, M. H. A. van Dongen, A. A. E. Stevens, J. van Geldrop, J. P. C. Bernards, *Appl. Surf. Sci.* **2014**, *290*, 381–387; b) L. Jiang, J. Liu, X. Lu, L. Fu, Y. Shi, J. Zhang, X. Zhang, H. Geng, Y. Hu, H. Dong, L. Jiang, J. Yu, W. Hu, *J. Mater. Chem. C* **2018**, *6*, 2419–2423.

[12] J. Huang, G. Zhang, X. Zhao, X. Wu, D. Liu, Y. Chu, H. E. Katz, *J. Am. Chem. Soc.* **2017**, *139*, 12366–12369.

Manuscript received: December 20, 2019
Accepted manuscript online: January 15, 2020
Version of record online: January 29, 2020

